White matter architecture in major depression with anxious distress symptoms

Heij, Gijs J; Penninx, Brenda W H J; van Velzen, Laura S; van Tol, Marie-José; van der Wee, Nic J A; Veltman, Dick J; Aghajani, Moji

Published in:
Progress in Neuro-Psychopharmacology & Biological Psychiatry

DOI:
10.1016/j.pnpbp.2019.109664

Publication date:
2019

Progress in Neuropsychopharmacology & Biological Psychiatry 94 (2019) 109664

Contents lists available at ScienceDirect

Progress in Neuropsychopharmacology & Biological Psychiatry

journal homepage: www.elsevier.com/locate/pnp

White matter architecture in major depression with anxious distress symptoms

Gijs J. Heij[a,b], Brenda W.H.J. Penninx[b,c], Laura S. van Velzen[b,c], Marie-José van Tol[d], Nic J.A. van der Wee[e], Dick J. Veltman[b,c], Moji Aghajani[b,c,*]

[a] VU University, Faculty of Earth and Life Sciences, the Netherlands
[b] Amsterdam UMC, Location VUMC, Dept. of Psychiatry & Amsterdam Neuroscience, the Netherlands
[c] GGZ InGeest Specialized Mental Health Care, the Netherlands
[d] University Medical Center Groningen, Dept. of Psychiatry, the Netherlands
[e] Leiden University Medical Center, Dept. of Psychiatry, the Netherlands

A B S T R A C T

Background: Comorbid anxious distress is common in Major Depressive Disorder (MDD), and associated with significantly worse clinical course and treatment response. While DSM-5 recently introduced the Anxious Distress (AD) specifier as a potentially useful symptom-based subtyping scheme for MDD, its neurobiological underpinnings remain unclear. The current study hence uniquely probed whether MDD with co-occurring AD (MDD/AD+) relates to distinct perturbations in frontolimbic white matter (WM) pathways tentatively theorized in MDD/AD+ pathophysiology.

Methods: Tract-based spatial statistics (TBSS) was therefore used to analyze diffusion tensor imaging data on WM microstructure, in MDD/AD+ patients (N = 20) relative to MDD patients without AD (MDD/AD-; N = 29) and healthy controls (HC; N = 39). Using TBSS, we probed fractional anisotropy and axial/radial/mean diffusivity as proxies for WM integrity. Categorical (between-groups) and dimensional (within-patients) analyses subsequently assessed how Anxious Distress in MDD impacts frontolimbic WM connectivity. Receiver-Operating Characteristics additionally assessed classification capabilities of between-groups WM effects.

Results: Compared to MDD/AD- and HC participants, MDD/AD+ patients exhibited diminished integrity within the anterior thalamic radiation (ATR). Higher AD specifier scores within MDD patients additionally related to diminished integrity of the uncinate fasciculus and cingulum pathways. These effects were not confounded by key clinical (e.g., comorbid anxiety disorder) and sociodemographic (e.g., age/sex) factors, with altered ATR integrity moreover successfully classifying MDD/AD+ patients from MDD/AD- and HC participants (90% sensitivity | 73% specificity | 77% accuracy).

Conclusions: These findings collectively link MDD/AD+ to distinct WM anomalies in frontolimbic tracts important to adaptive emotional functioning, and may as such provide relevant, yet preliminary, clues on MDD/AD+ pathophysiology.

1. Introduction

Major Depressive Disorder (MDD) is one of the most prevalent and debilitating psychiatric disorders, affecting hundreds of millions of people worldwide (WHO, 2017). Despite these concerns, a significant portion of MDD patients do not fully benefit from currently available treatment options and are severely impaired by MDD symptomatology (Lener and Iosifescu, 2015). Many scholars and clinicians point to the unitary diagnosis of MDD, based on heterogeneous symptom profiles, as one of the main reasons for our inability to fully understand MDD pathophysiology and formulate targeted, personalized treatments. To address this issue and encourage subtype-specific research and treatment initiatives, the newly revised *DSM-5* included several specifiers for the diagnosis of MDD, aimed at meaningful subgrouping of MDD patients based on etiology, symptomatology, and treatment responsivity (APA, 2013; Gaspersz et al., 2018; Ionescu et al., 2013).

One specifier that seems of particular clinical relevance, and has thus far received the most attention, is the "Anxious Distress" (AD) specifier (Gaspersz et al., 2017a; Gaspersz et al., 2017b; Gaspersz et al., 2017; Gaspersz et al., 2018; Ionescu et al., 2013; Kessler et al., 2015). This specifier describes a subgroup of MDD patients who in addition to their depressive symptoms also feel keyed up, tense, and restless, have difficulty concentrating/focusing because of excessive worrying and anxiousness, and often fear that they could lose control (APA, 2013). Data suggest that 50–65% of MDD patients would meet the criteria for AD, with the specifier additionally outperforming comorbid anxiety diagnoses in predicting important clinical outcomes (e.g., chronicity, remission, disability), thus highlighting its presumed clinical relevance (Gaspersz et al., 2017a; Gaspersz et al., 2017b; Ionescu et al., 2013; Rosellini et al., 2018). Studies moreover show that MDD with co-occurring AD (MDD/AD+) versus MDD without AD (MDD/AD-) often has an earlier age of onset, is more severe in its symptomatology, relates to

* Corresponding author at: Amsterdam UMC/VUMC, Department of Psychiatry, Oldenaller 1, 1081 HJ Amsterdam, the Netherlands.
E-mail address: m.aghajani@vumc.nl (M. Aghajani).

https://doi.org/10.1016/j.pnpbp.2019.109664
Received 3 January 2019; Received in revised form 29 April 2019; Accepted 30 May 2019
Available online 31 May 2019

less favorable treatment prognosis and remission rates, and includes more antidepressant side effects (Gaspersz et al., 2017a; Gaspersz et al., 2017b; Kessler et al., 2015). These differences are deemed reminiscent of distinct neurobiological underpinnings (Albaugh et al., 2017a; Canu et al., 2015; Gaspersz et al., 2017a; Gaspersz et al., 2017b; Gaspersz et al., 2018; Potvin et al., 2015; Zhao et al., 2017), and uncovering them seems particularly important for improving diagnosis, prognosis, and treatment (Ionescu et al., 2013).

There is some evidence indeed for this premise (though not always unequivocal: e.g., Gaspersz et al., 2018; van Tol et al., 2010), with more severe cortical thinning, frontolimbic circuit dysfunction, immunological imbalance, and cellular disintegrity being reported in MDD patients with co-occurring AD symptoms (Albaugh et al., 2017b; Gaspersz et al., 2017a; Gaspersz et al., 2018; Ionescu et al., 2013; Zhao et al., 2017). The proposed frontolimbic circuit dysfunction is of particular interest, given its established role in abnormal emotion processing/regulation and affective psychopathology (Caetano et al., 2007; Disner et al., 2011; Mayberg, 2003; Phillips et al., 2015; Phillips et al., 2008; Price and Drevets, 2010). This frontolimbic circuit comprises various prefrontal subregions and key limbic structures such as the amygdala, hippocampus and striatum, which together form an integrated neural circuit dedicated to various aspects of emotion processing and regulation. Within this circuit, the amygdala, striatum, subgenual/ventral anterior cingulate cortex (ACC), ventrolateral prefrontal cortex (PFC), and orbitofrontal cortex (OFC) form a ventral frontolimbic system, which encodes the emotional significance of a stimulus and produces an affective response to it (Phillips et al., 2015; Phillips et al., 2008; Stein et al., 2007). The dorsal ACC, dorsomedial PFC, dorsolateral PFC, and hippocampus, on the other hand, are implicated in a dorsal system that exerts cognitive control, regulates affective states, and provides contextual information (Pessoa, 2008; Phillips et al., 2015; Phillips et al., 2003; Phillips et al., 2008; Stein et al., 2007). There is evidence for a functional imbalance between and within these frontolimbic systems (Bhatia et al., 2018; Phillips et al., 2008; Phillips et al., 2003; Price and Drevets, 2010), which are deemed partly driven by microstructural changes in white matter (WM) bundles of the uncinate fasciculus (UNC) and cingulum (CIN) that crucially interlink key nodes of these systems (Bhatia et al., 2018; Bracht et al., 2015; Cullen et al., 2010; Phillips et al., 2008; Phillips et al., 2015; Phillips et al., 2003).

The UNC is a long-range WM tract that connects key limbic regions such as the amygdalar and hippocampal complexes in the anterior temporal lobe to ventral frontal lobe territories, including ventromedial/orbitofrontal sections of the PFC and ventral ACC regions (Olson et al., 2015). The location and connectivity profile of the UNC pinpoint it as an integral component of adaptive frontolimbic interactions, and abnormalities in its structural integrity are often linked to abnormal emotional processing and susceptibility to affective psychopathology (Bracht et al., 2015; Cullen et al., 2010; LeWinn et al., 2014; Olson et al., 2015; Sexton et al., 2009; Von Der Heide et al., 2013). The CIN bundle, on the other hand, allows for more widely-distributed interconnections by linking prefrontal, cingulate, parietal and medial temporal sites, whilst also interlinking key subcortical nuclei (e.g., thalamic nuclei) to various cingulate regions (Bubb et al., 2018; Wu et al., 2016). It is involved in a wide range of processes, such as emotion processing, motivational drive, executive functioning, pain and memory (Bubb et al., 2018). It is noteworthy that studies indicative of UNC microstructural alterations in MDD also implicate involvement of the CIN in MDD pathophysiology (Bhatia et al., 2018; Bracht et al., 2015; Cullen et al., 2010), further corroborating the crucial role of both tracts in mood dysregulation (Bhatia et al., 2018; Keedwell et al., 2012; Keedwell and Linden, 2013; Sexton et al., 2009). However, whether specific alterations in UNC and CIN microstructure may also relate to MDD/AD+ diagnosis, symptomatology, and severity has yet to be investigated.

It is worth mentioning that altered WM microstructure is also found in pathways other than UNC and CIN among MDD patients, with some alterations even occurring early in the course of MDD (Aghajani et al., 2014; Zhu et al., 2011). Commonly affected pathways include the corpus callosum, superior/inferior longitudinal fasciculus, forceps, internal capsule, and anterior thalamic radiation, with generally lower integrity of WM bundles being reported (Bracht et al., 2015; Dillon et al., 2018; Jiang et al., 2017; Liao et al., 2013; Shen et al., 2017; Wen et al., 2014). It should be noted though that WM findings in MDD are not always unequivocal, with several important studies reporting opposing effects or even null findings (e.g., see meta-analysis Choi et al., 2014). These mixed findings might, among other things, be ascribed to the heterogeneous nature of MDD, with various subgroups of patients presenting different etiology, symptomatology, and treatment responsivity profiles (Belmaker and Agam, 2008). A subtype-specific approach towards MDD is therefore anticipated to tackle these conflicting findings, improve our understanding of underlying neurobiology, and aid personalized treatment. That said, little is yet known of whether *DSM-5 informed* MDD subtypes, and in particular MDD/AD+, may involve specific WM anomalies. A handful of studies have tried to address this issue, though fairly indirectly by either using a AD specifier not conforming to *DSM-5* criteria or comparing MDD patients with vs. without comorbid anxiety on WM integrity (e.g., Delaparte et al., 2017; Xia et al., 2018). However, MDD with comorbid anxiety disorder tends to capture a partially different group of patients than MDD/AD+ (Gaspersz et al., 2017a; Rosellini et al., 2018), as evidenced by the poor overlap between the presence of the AD specifier and comorbid anxiety disorders among MDD patients (Gaspersz et al., 2017a). The DSM-5 informed AD specifier is additionally deemed more useful than comorbid anxiety diagnoses in formulating meaningful MDD subtypes, partly due to its higher discriminative power on key clinical outcomes (Gaspersz et al., 2017a; Gaspersz et al., 2018; Rosellini et al., 2018). Examining WM microstructure in MDD/AD+ patients thus seems rather pertinent, as it may provide deeper insights into the underlying neuropathology and aid biomarker development in the future.

We therefore employed tract-based spatial statistics (TBSS: Smith et al., 2006) to analyze diffusion tensor imaging (DTI) data on WM microstructure, in MDD/AD+ patients relative to MDD/AD- and healthy control (HC) participants. Our main parameter of interest was fractional anisotropy (FA), which reflects the tendency of water molecules in WM to diffuse in one direction as opposed to all other directions, thereby providing a *general proxy* for WM microstructural integrity (e.g., myelin thickness, membrane integrity) (Kochunov et al., 2007). FA, however, is less informative about the specific type of alterations that may present in WM fiber bundles, so additional parameters are commonly calculated and examined to gain more insight in underlying mechanisms (Alexander et al., 2007). We therefore additionally probed axial (A.Dif), radial (R.Dif), and mean (M.Dif) diffusivity, which provide complementary information on axonal integrity, fiber bundle coherence, and myelination, thereby aiding interpretation of FA changes (Alexander et al., 2007; Budde et al., 2009; Horsfield and Jones, 2002; Song et al., 2002) (see Fig. 1 for schematic representation). Specifically, A.Dif indexes water diffusion along the principal direction of the fiber, and is deemed sensitive to axonal integrity and fiber bundle coherence. R.Dif tends to index diffusion perpendicular to the principal direction of the fiber, and is more indicative of myelination level. Finally, M.Dif reflects average water diffusion in all directions within the fiber bundle, providing a proxy marker for cellularity.

Given the proposed frontolimbic circuit dysfunction in MDD (Disner

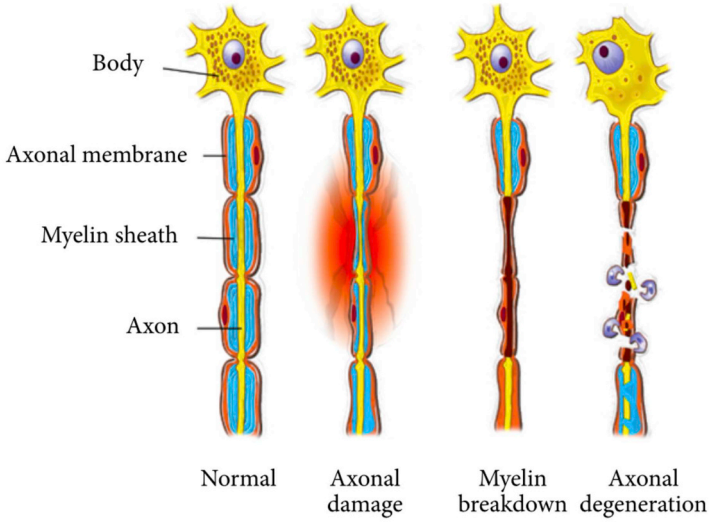

(A)

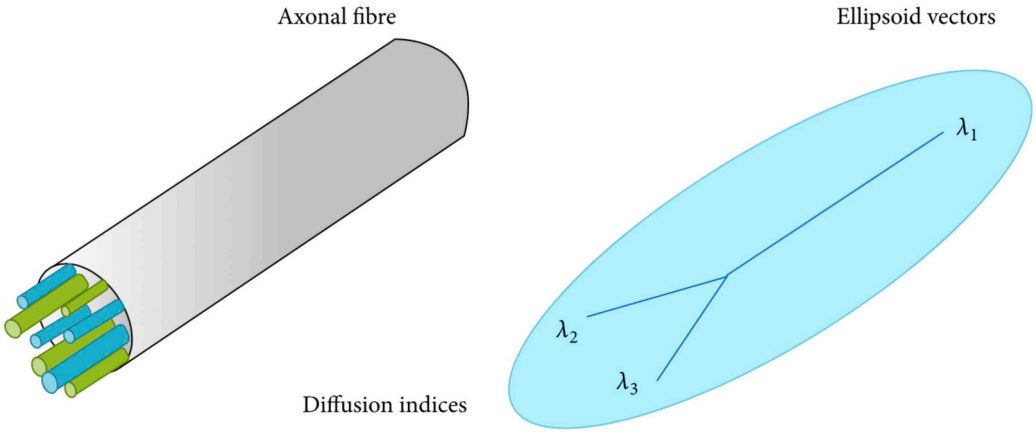

$$FA = \sqrt{\frac{1}{2}} \cdot \frac{\sqrt{(\lambda_1 - \lambda_2)^2 + (\lambda_2 - \lambda_3)^2 + (\lambda_3 - \lambda_1)^2}}{\sqrt{(\lambda_1)^2 + (\lambda_2)^2 + (\lambda_3)^2}} \quad M.Dif = \left(\frac{\lambda_1 + \lambda_2 + \lambda_3}{3}\right) \quad R.Dif = \left(\frac{\lambda_2 + \lambda_3}{2}\right) \quad A.Dif = (\lambda_1)$$

(B)

DTI Index				
Characteristic	**FA**	**A.Dif**	**R.Dif**	**M.Dif**
Diffusivity	In one direction as opposed to all other directions	Along the principal direction of the fiber	Perpendicular to the principal direction of the fiber	Average water diffusion in all directions within the fiber
Tissue Proxy	General WM integrity	Axonal integrity	Myelination level	Cellularity level

(C)

Fig. 1. Schematic representation of key DTI indices and their properties. The upper panel (A) depicts key neural tissue properties within WM that DTI allows to approximate in vivo. The middle and lower panel (B, C) depict the physics behind DTI. DTI measures the magnitude and orientation of water diffusion within axonal fiber bundles. It uses measures derived from the three eigenvectors, represented by their eigenvalues (λ1, λ2, λ3), which define the diffusion ellipsoid/tensor in every voxel. FA reflects the general tendency of water molecules in WM to diffuse in one direction as opposed to all other directions. A.Dif (λ1) indexes water diffusion along the principal direction of the fiber, whereas R.Dif ((λ2 + λ3)/2) reflects diffusion perpendicular to the principal direction of the fiber, with M.Dif ((λ1 + λ2 + λ3)/3) indexing average water diffusion in all directions within the fiber bundle. Whereas FA provides a general proxy for WM microstructural integrity, A.Dif is deemed sensitive to axonal integrity and fiber bundle coherence, R.Dif to myelination level, and M.Dif to cellularity levels. DTI = Diffusion Tensor Imaging; WM = White Matter; FA = Fractional Anisotropy; A.Dif = Axial Diffusivity; R.Dif = Radial Diffusivity; M.Dif = Mean Diffusivity. Reprinted with permission from Hindawi Publishing Corporation: BioMed Research International, (Alves et al., 2015).

et al., 2011; Mayberg, 2003; Phillips et al., 2015; Price and Drevets, 2010) and the relevance of UNC and CIN bundles to frontolimbic connectivity (Cohen et al., 2008; Concha et al., 2005; Petrides and Pandya, 2002; Swartz and Monk, 2014), we focused primarily on these two WM tracts. For completeness though, we also performed whole-brain analyses to capture potential WM changes in other tracts, including those considered pertinent to adaptive frontolimbic communication and affective psychopathology (e.g., anterior thalamic radiation, forceps minor, and internal capsule) (Bracht et al., 2015; Dillon et al., 2018; Jiang et al., 2017; Liao et al., 2013; Shen et al., 2017; Wen et al., 2014). We employed categorical between-groups (based on the presence of the AD specifier) and dimensional within-patient analyses (based on the total AD specifier score) to thoroughly examine the impact of the AD specifier on WM architecture in MDD patients. We hypothesized diminished WM integrity as indexed by lower FA values among MDD/AD + patients versus MDD/AD- and HC participants, with these group differences following a linear trend (MDD/AD + < MDD/AD- < HC), echoing the more severe symptomatology and neuropathology of MDD/AD + (Gaspersz et al., 2017b; Gaspersz et al., 2017; Gaspersz et al., 2018; Kessler et al., 2015). We additionally speculated that higher AD specifier total scores in MDD patients would relate to lower FA values. Post-hoc analyses moreover probed the impact of key clinical and sociodemographic factors on potential WM changes, and additionally assessed whether the presence of the AD specifier vs. comorbid anxiety disorders relates to distinct/overlapping WM alterations. Receiver-Operating Characteristics were finally computed to assess diagnostic sensitivity of between-groups (categorical) WM effects in classifying MDD/AD + patients from MDD/AD- and HC participants.

2. Methods and materials

2.1. Participants

The current sample comprised a subset from the most recent wave (9-year follow-up) of the Netherlands Study of Depression and Anxiety (NESDA) (Penninx et al., 2008), and only included MDD and HC participants who had complete DTI datasets and sufficient data to formulate the AD specifier (N = 91). Visual inspection and quality control of DTI data resulted in exclusion of 3 participants due to: missing DTI scan in anterior-to-posterior direction (1), differing gradients in the anterior-to-posterior and posterior-to-anterior DTI scan (1), and missing volumes in the posterior-to-anterior DTI scan (1). The dataset of 88 subjects consisted of 49 patients with current MDD diagnosis (mean age = 48.98, *SD* = 8.57; 49% female) and 39 HC participants (mean age = 52.10, *SD* = 8.44; 39% female). The groups were matched on age, sex, and education. MDD patients were recruited through general practitioners, primary care, and specialized mental care institutions, while HC participants were approached via local advertisements. DSM diagnoses of current (6-month recency) MDD were established using the Composite International Diagnostic Interview lifetime version 2.1 (Andrews and Peters, 1998).

Patients were excluded if they presented Axis I disorders other than MDD or anxiety disorder (i.e., panic disorder, social anxiety disorder and/or generalized anxiety disorder), and used psychotropic medications other than selective serotonin reuptake inhibitors (SSRIs) on a stable basis or benzodiazepine on an infrequent basis (oxazepam/diazepam, maximum of three times a week, max 10 mg, and not within 48 h before scanning). Exclusion criteria for HC participants were lifetime diagnosis of MDD or other psychopathologies, and use of any psychotropic medication, with the exception of infrequent benzodiazepine use (< 1 days per week). All participants were asked not to use benzodiazepines or recreational drugs in the 48 h preceding the scan. Exclusion criteria for the entire group were: the presence or history of major internal or neurological disorder, dependency or recent abuse (past year) of alcohol or drugs, hypertension, severe head trauma, insulin dependence, presence of MRI-contraindications, and not being fluent in Dutch language. Ethical Review Boards of the three participating centers (VU Medical Center = VUMC; Leiden University Medical Center = LUMC; University Medical Center Groningen = UMCG) approved this study, and written informed consent was obtained from all participants. Detailed information on sample characteristics is provided in Table 1.

3. Anxious distress specifier

As per prior work (Gaspersz et al., 2017a; Gaspersz et al., 2017b; Gaspersz et al., 2017; Gaspersz et al., 2018), the AD specifier for MDD patients was constructed based on 5 self-reported items from the Inventory of Depressive Symptomatology (IDS (Rush et al., 1996)) and the Beck Anxiety Inventory (BAI (Beck et al., 1988)). These items directly matched with the *DSM-5* criteria for the AD specifier: (1) feeling keyed up or tense (IDS item 7); (2) feeling unusually restless (IDS item 24); (3) difficulty concentrating because of worry (IDS item 15); (4) fear that something awful might happen (BAI item 5); (5) feeling that the individual might lose control of self (BAI item 14). Both questionnaires assess symptoms in the past week on a 0–3 (not at all-to-severe) scale, and symptoms are considered present when a patient indicates a score ≥2 (i.e., moderate or severe). The presence of the specifier was assessed according to the criterion of the *DSM-5*, requiring that the MDD patient presents/fulfills at least 2 of 5 the symptoms. In addition to this dichotomous approach (i.e., specifier was present or absent), we also examined the total specifier severity score (sum score of 5 AD items: 0–15) for *within-patients* examination of WM. Earlier studies (Gaspersz et al., 2017a; Gaspersz et al., 2017b) have shown that the AD specifier has an adequate internal consistency (Crohnbach's $\alpha = 0.71$) and predictive validity for subsequent course and treatment response in depressed patients (Gaspersz et al., 2018). Based on the criteria mentioned above, 20 of the 49 MDD patients met the criteria for the AD specifier (see Table 1 for characteristics).

4. DTI data acquisition and preprocessing

Participants were scanned at one of the three participating centers: VUMC (N = 41), LUMC (N = 29), and UMCG (N = 18). DTI data were collected using a Philips 3 T MRI scanner (Philips Medical Systems, The Netherlands) with a 32-channel phased array head coil. A single-shot echo-planar imaging (EPI) sequence was used with the following parameters: TR = 7351 ms, TE = 71 ms, flip angle = 90°, *b* factor = 1000 s/mm^2, FOV = 240 × 240 × 150 mm, voxel dimensions = 1.88 × 2.35 × 2.00 mm, number of transverse slices = 75, and no slice gap. DTI data were acquired along 32 directions, together with a baseline image having no diffusion weighting ($b = 0$). Data was collected with reversed phase-encode directions, resulting in pairs of images with distortions going in opposite directions. The total scanning time was approximately 8 min: 4 min acquisition in anterior to posterior direction and 4 min posterior to anterior direction. Collected DTI data were preprocessed and analyzed using FSL version 5.0.10. (https://fsl.fmrib.ox.ac.uk/fsl/fslwiki/FSL) (Smith et al., 2004).

After visual inspection of the data and quality control, FSL's Topup Tool (Andersson et al., 2003; Smith et al., 2004; Van Essen et al., 2012) was used to estimate susceptibility-induced off-resonance field maps based on the b0-images and acquisition parameters. These off-resonance field maps - together with brain-extracted mask images - were then fed into FSL's Eddy Tool (Andersson and Sotiropoulos, 2016) to correct for distortion and motion artefacts induced by eddy currents or

Table 1
Characteristics of the sample.

Characteristic				Difference
	MDD/AD + (N = 20)	MDD/AD-(N = 29)	HC (N = 39)	
Age, Years [a]	50.25 ± 6.66	48.10 ± 9.69	52.10 ± 8.44	
Sex, N (%) [a]				
Female	9 (45)	8 (28)	19 (49)	
Male	11 (55)	21 (72)	20 (51)	
Education (years) [a]	13.65 ± 2.74	13.03 ± 3.11	14.15 ± 2.93	
Scan Location, n (%) [a]				
Amsterdam	8 (45)	7 (55.2)	10 (41)	
Leiden	5 (20)	17 (31)	21 (41)	
Groningen	7 (35)	5 (13.8)	8 (18)	
IDS [b]	34.05 ± 10.69	23.0 ± 8.43	4.38 ± 4.27	1 > 2 > 3
BAI [b]	16.45 ± 7.31	9.17 ± 6.34	1.74 ± 2.67	1 > 2 > 3
AD Specifier Total [b]	11.60 ± 1.27	8.21 ± 1.69	5.36 ± 0.74	1 > 2 > 3
IDS-Atypical [b]	6.10 ± 3.11	5.17 ± 2.24	0.77 ± 1.25	1 = 2 > 3
IDS-Melancholic [b]	9.77 ± 4.87	6.71 ± 4.03	1.05 ± 1.73	1 > 2 > 3
Antidepressants [c]				
SSRI	5	8	–	
TCA	1	1	–	
Comorbidity [a,c]				
Social Phobia	4	3	–	
Panic Disorder	2	2	–	
GAD	3	4	–	
Mixed	1	2	–	

MDD = Major Depressive Disorder; MDD/AD + = MDD with Anxious Distress; MDD/AD- = MDD without Anxious Distress; HC = Healthy Controls; IDS = Inventory of Depressive Symptomatology; BAI = Beck Anxiety Inventory; AD Specifier Total = sum score on 5 IDS and BAI items (range 0–15); IDS-Atypical = atypical symptoms scale; IDS-Melancholic = melancholic symptoms scale; SSRI = selective serotonin reuptake inhibitors; TCA = tricyclic antidepressants; GAD = generalized anxiety disorder; Mixed = multiple comorbid anxiety disorders.
Values are given as mean ± standard deviation or number. Categorical variables (sex, scan location, medication, and presence of comorbid anxiety disorder) were tested using Chi-square test, whereas continuous variables were tested with nonparametric Kruskal-Wallis ANOVA (IDS, BAI, and AD Specifier Total) or parametric ANOVA (age, education).
[a] Not significant ($P > 0.05$).
[b] Significant at $P < 0.001$.
[c] Only tested within-patients, not applicable to HC participants.

by simple head motions. To correct for movement that coincided with the diffusion encoding part of the sequence (causing partial or complete signal dropout), FSL's Outlier Replacement Tool (Andersson et al., 2016) was additionally used, which detects dropout-slices and replaces them with Gaussian Process prediction. Finally, to generate individual FA, A.Dif, R.Dif and M.Dif maps for each participant, the standard diffusion tensor model was fitted to each voxel using FSL's Diffusion Toolbox (Behrens et al., 2003). A.Dif was defined as the largest eigenvalue vector ($\lambda 1$), R.Dif was calculated as the average of the two small eigenvalues ($(\lambda 2+\lambda 3)/2$), and M.Dif was calculated as the average of the three eigenvalues ($(\lambda 1+\lambda 2+\lambda 3)/3$) (https://fsl.fmrib.ox.ac.uk/fsl/fslwiki/TBSS). Whereas A.Dif is deemed sensitive to axonal integrity and fiber bundle coherence, R.Dif is more indicative of myelination level, with M.Dif providing a proxy marker for cellularity (Alexander et al., 2007)

5. TBSS analyses

Tract-based spatial statistics (TBSS) (Smith et al., 2006) version 1.2 was used for voxelwise analyses of the preprocessed DTI data. First, all individual FA images were aligned to the FMRIB58_FA standard-space image using FMRIB's non-linear registration tool (FNIRT). Next, a mean FA image was created and skeletonized, representing the centers of all major tracts common to the entire group. This skeleton was then thresholded at an FA value of 0.35 to exclude peripheral tracts and minimize partial voluming (Aghajani et al., 2014; Westlye et al., 2009). Finally, each participant's aligned FA images were projected onto the mean FA skeleton. In a similar manner, A.Dif, R.Dif and M.Dif data were projected onto the skeleton using the FA registration and skeleton projection parameters. In line with prior work, FA was examined throughout the WM skeleton, while A.Dif, R.Dif and M.Dif were only examined in regions showing significant FA changes to aid interpretation of these changes.

To test for regional specific FA alterations in UNC and CIN, bilateral masks for these tracts were first created as per prior work (Aghajani et al., 2014; Westlye et al., 2011; Westlye et al., 2009), using the probabilistic Johns Hopkins University and Juelich Histological WM atlases (Eickhoff et al., 2007; Mori et al., 2005) provided by FSL. The UNC and CIN masks were then skeletonized against the thresholded mean FA skeleton to include only voxels comprised in the individual masks and the mean skeleton. This confines the statistical analyses to voxels from the center of the tract, thereby minimizing anatomic inter-subject variability, registration errors and partial voluming (Aghajani et al., 2014; Westlye et al., 2009). The resulting UNC and CIN masks were subsequently used for voxel-wise permutation-based statistical analyses. For completeness, we also performed whole-brain voxel-wise analyses to capture potential WM changes in other tracts, including those considered pertinent to adaptive frontolimbic communication and affective psychopathology (e.g., anterior thalamic radiation, forceps minor, and internal capsule) (Bracht et al., 2015; Dillon et al., 2018; Jiang et al., 2017; Liao et al., 2013; Shen et al., 2017; Wen et al., 2014).

The statistical inferences included both a *categorical - between-groups*

- approach (based on the presence of the AD specifier) and a *dimensional - within-patients* - approach (based on the total AD specifier score) to thoroughly examine the impact of the AD specifier on WM architecture in MDD patients. The categorical between-groups analysis comprised MDD/AD+, MDD/AD-, HC participants, and probed whether MDD/AD + involves diminished FA values compared to MDD/AD- and HC, according to a linear trend (MDD/AD+ < MDD/AD- < HC). The dimensional within-patients analysis included only the MDD patients and probed whether higher AD specifier total scores (mean-centered) among individual patients would relate to lower FA values. Statistical analyses were performed using FSL's permutation-based Randomise tool, which included 5000 random permutations to build up the null distribution of the cluster size statistic, while testing our contrasts of interest in the categorical and dimensional analyses. Statistical maps were thresholded using threshold-free cluster enhancement (TFCE (Smith and Nichols, 2009)) with cluster normalization (Salimi-Khorshidi et al., 2011), and family-wise error (FWE) corrected for multiple comparisons at $P < 0.05$.

Post-hoc analyses probed whether adjusting for antidepressant use, current comorbid anxiety disorders, presence of melancholic and atypical MDD symptoms (bases on IDS items: Gaspersz et al., 2017; Khan et al., 2006; Novick et al., 2005), sociodemographics (age, sex, education), and scan location might impact any of the emerging findings (all covariates mean-centered). Post-hoc analyses additionally assessed whether the presence of the AD specifier vs. current comorbid anxiety disorders may relate to distinct or overlapping WM correlates. Finally, to explore the sensitivity and specificity of between-groups (i.e., categorical) WM effects in classifying MDD/AD+ patients versus MDD/AD- and HC participants, Receiver-Operating Characteristics (ROC) analyses were conducted.

6. Results

6.1. Sample characteristics

As shown in Table 1, MDD/AD+ patients did not differ in age, sex, education and scan location from MDD/AD- and HC participants. Kruskal-Wallis ANOVA revealed a linear trend in which MDD/AD+ patients scored the highest on the IDS, BAI and AD specifier total, followed by MDD/AD- and HC, respectively. Of note, the three groups still differed on the AD specifier total scores when correcting for melancholic and atypical symptoms (univariate model: $F(2,83) = 59.43$, $P < 0.001$), further showcasing the robustness and specificity of the AD construct in the current study. Finally, MDD/AD+ and MDD/AD- patients did not differ in terms of antidepressant use and presence of current comorbid anxiety disorders (P's > 0.05).

6.2. TBSS analysis

6.2.1. Categorical approach

The categorical analyses focusing on UNC and CIN microstructure revealed no significant between-groups differences in FA within these

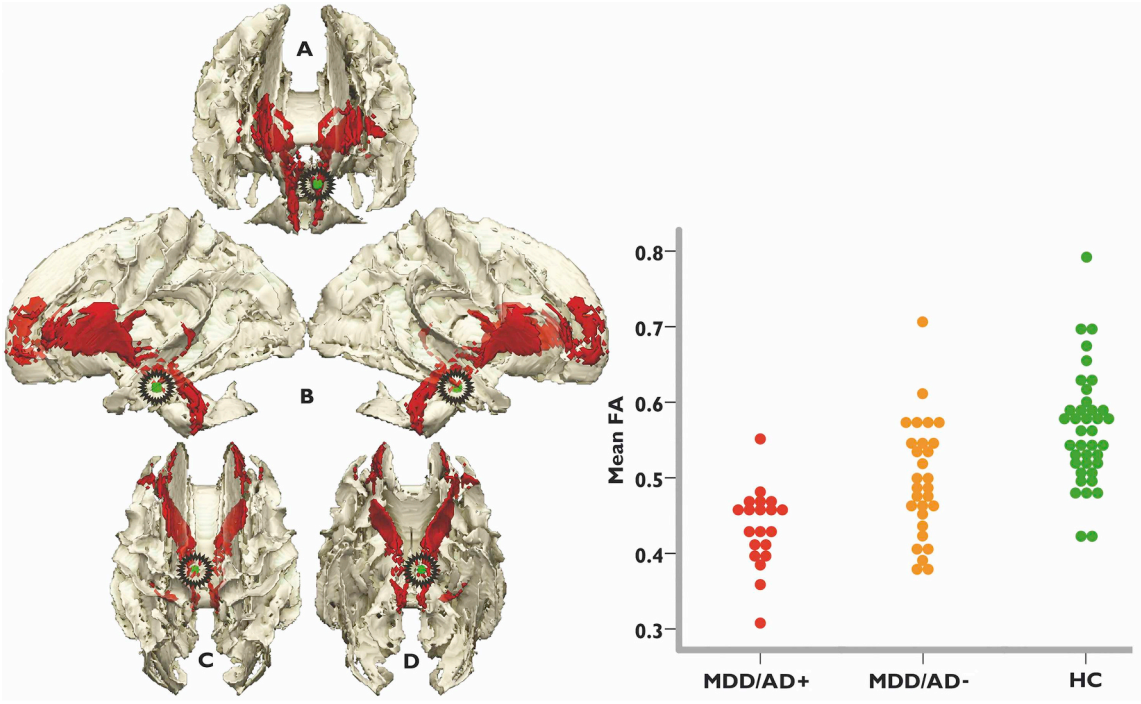

Fig. 2. MDD/AD+ relates to diminished ATR integrity. The left panel depicts anterior (A), lateral (B), superior (C), and inferior (D) views of the WM skeleton (beige/grey) and the ATR tract (red), with a subregion of the ATR (green) showing significantly reduced FA in MDD/AD+ patients relative to MDD/AD- and HC participants, respectively (P = 0.01, *TFCE* and *FWE* corrected). Closer examination revealed that the effect site was in the vicinity of the brainstem/substantia nigra region, in which the change in FA was mainly driven by increased A.Dif, R.Dif, M.Dif levels among MDD/AD+ patients relative to MDD/AD- and HC participants, respectively (P's < 0.01, *TFCE* & *FWE* corrected). Black edged circles mark the effect site for better visibility. The distribution plot (right panel) provides a quantitative visualization of the effect, wherein mean FA estimates from the effect site (y axis) are plotted for each group (x axis). MDD/AD+ = Major Depressive Disorder *with* Anxious Distress; MDD/AD- = Major Depressive Disorder *without* Anxious Distress; HC = Healthy Controls; ATR = Anterior Thalamic Radiation; WM = White Matter; FA = Fractional Anisotropy; TFCE = Threshold Free Cluster Enhancement; FWE = Family-Wise Error; A.Dif = Axial Diffusivity; R.Dif = Radial Diffusivity; M.Dif = Mean Diffusivity. (For interpretation of the references to colour in this figure legend, the reader is referred to the web version of this article.)

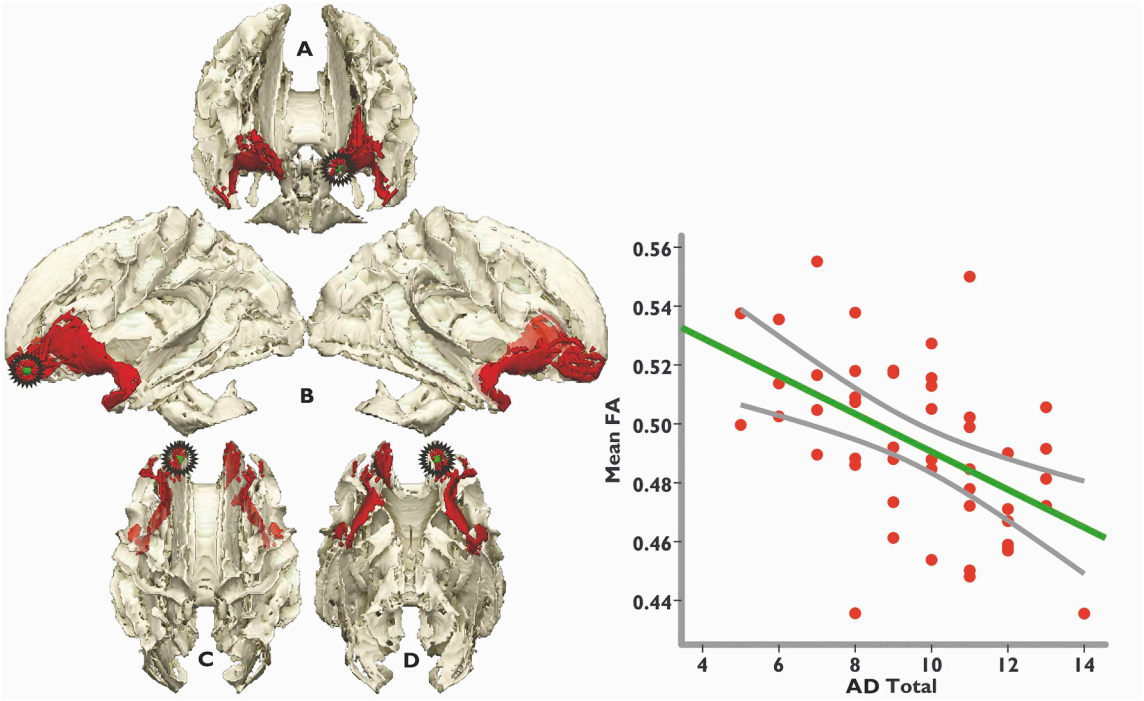

Fig. 3. Higher AD specifier total scores relate to diminished UF integrity. The left panel depicts anterior (A), lateral (B), superior (C), and inferior (D) views of the WM skeleton (beige/grey) and the UNC tract (red), with a subregion of the UNC (green) showing significantly reduced FA in MDD patients, as a function of higher AD specifier scores ($P < 0.02$, *TFCE* & *FWE* corrected). Closer examination revealed that the effect site was in the orbitofrontal regions, in which the change in FA was mainly driven by decreased A.Dif, increased R.Dif, and preserved M.Dif (P's < 0.01, *TFCE* & *FWE* corrected). Black edged circles mark the effect site for better visibility. The scatter plot (right panel) provides a quantitative visualization of the effect, wherein mean FA estimates from the effect site (y axis) are plotted against the AD specifier total scores (x axis). The green line depicts the slope of the association, with the grey bands indicating the 99% confidence interval of the slope. AD = Anxious Distress Specifier; MDD = Major Depressive Disorder UNC = Uncinate Fasciculus; WM = White Matter; FA = Fractional Anisotropy; TFCE = Threshold Free Cluster Enhancement; FWE = Family-Wise Error; A.Dif = Axial Diffusivity; R.Dif = Radial Diffusivity; M.Dif = Mean Diffusivity. (For interpretation of the references to colour in this figure legend, the reader is referred to the web version of this article.)

tracts. Complementary whole-brain TBSS analysis, however, revealed a significant FA effect within the left anterior thalamic radiation (ATR), wherein MDD/AD+ patients exhibited the lowest FA values in comparison to MDD/AD- and HC participants, respectively ($P = 0.01$, *TFCE* and *FWE* corrected) (see Fig. 2). Closer examination revealed that the effect site was in the vicinity of the brainstem/substantia nigra region, in which the change in FA was mainly driven by higher A.Dif, R.Dif, and M.Dif levels among MDD/AD+ patients relative to MDD/AD- and HC participants, respectively (P's < 0.01, *TFCE* & *FWE* corrected). No other effects emerged from these between-group analyses.

6.2.2. Dimensional approach

The dimensional within-patient analysis, however, did reveal an association between MDD patients' AD specifier total scores and UNC and CIN microstructure. Specifically, higher AD scores related to lower FA values in the OFC section of the left UNC and ventral ACC segment of the right CIN (P's < 0.02, *TFCE* & *FWE* corrected) (see Fig. 3 & Fig. 4). Examination of diffusivity measures revealed that these changes in FA were both mainly driven by decreased A.Dif, increased R.Dif, and preserved M.Dif (P's < 0.01, *TFCE* & *FWE* corrected). Patients' AD specifier scores were not associated with elevated FA levels, nor were any associations found between AD scores and FA in other WM tracts (i.e., complementary whole-brain analysis).

6.2.3. Confound correction

Similar to prior work (e.g., Cullen et al., 2014; Roy et al., 2013), individual participants' mean FA from regions of significant effect were used as dependent variable in a series of post-hoc analyses (SPSS, Version 25, IBM Corp., Armonk, N.Y., USA), which probed the impact of antidepressant use and comorbidity, along with sociodemographics (age, sex, education) and scan location, on FA changes documented here. Analyses of variance (ANOVA's) revealed that the categorical between-group effect within the ATR remained significant when excluding MDD patients who were on antidepressants (N = 16 excluded) (univariate model: $F(2,71) = 11.49$, $P < 0.05$; Linear Contrast: 95% CI = −0.10–−0.04, $P < 0.05$) or had a current comorbid anxiety disorder (N = 21 excluded) (univariate model: $F(2,64) = 6.37$, $P < 0.05$; Linear Contrast: 95% CI = −0.10–−0.03, $P < 0.05$). Including all participants and covarying for antidepressant use, comorbidity, melancholic and atypical MDD symptoms, sociodemographics (age, sex, education), and scan location similarly did not affect the documented ATR effect (univariate model: $F(2,76) = 3.54$, $P < 0.05$; Linear Contrast: 95% CI = −0.08–−0.05, $P < 0.05$). Multiple regression analyses furthermore revealed that the dimensional within-patients effects in the UNC and CIN remained significant when excluding MDD patients who were on antidepressants (N = 16 excluded) (UNC: $\beta = -0.50$, $P < 0.05$; CIN: $\beta = -0.55$, $P < 0.05$) or

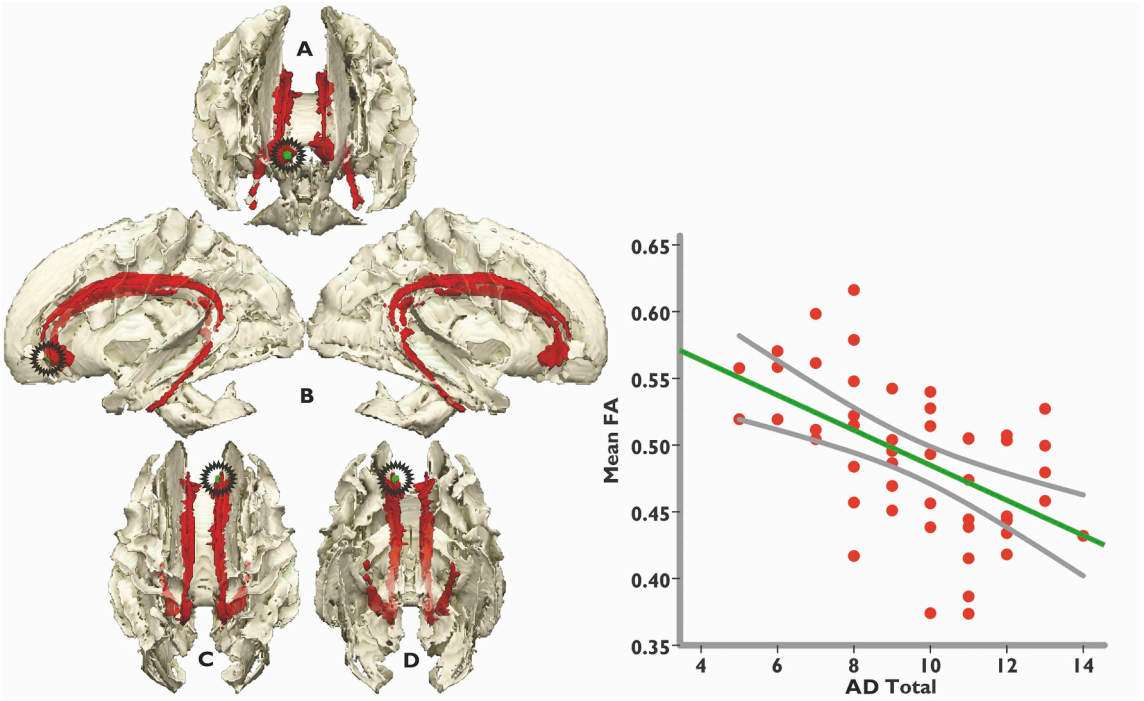

Fig. 4. Higher AD specifier total scores relate to diminished CIN integrity. The left panel depicts anterior (A), lateral (B), superior (C), and inferior (D) views of the WM skeleton (beige/grey) and the CIN tract (red), with a subregion of the CIN (green) showing significantly reduced FA in MDD patients, as a function of higher AD specifier total scores ($P < 0.02$, *TFCE* & *FWE* corrected). Closer examination revealed that the effect site was in the ventral anterior cingulate region, in which the change in FA was mainly driven by decreased A.Dif, increased R.Dif, and preserved M.Dif (P's < 0.01, *TFCE* & *FWE* corrected). Black edged circles mark the effect site for better visibility. The scatter plot (right panel) provides a quantitative visualization of the effect, wherein mean FA estimates from the effect site (y axis) are plotted against the AD specifier total scores (x axis). The green line depicts the slope of the association, with the grey bands indicating the 99% confidence interval of the slope. AD = Anxious Distress Specifier; MDD = Major Depressive Disorder CIN = Cingulum; WM = White Matter; FA = Fractional Anisotropy; TFCE = Threshold Free Cluster Enhancement; FWE = Family-Wise Error; A.Dif = Axial Diffusivity; R.Dif = Radial Diffusivity; M.Dif = Mean Diffusivity. (For interpretation of the references to colour in this figure legend, the reader is referred to the web version of this article.)

had a comorbid anxiety disorder (N = 21 excluded) (UNC: $\beta = -0.55$, $P < 0.05$; CIN: $\beta = -0.52$, $P < 0.05$). Including all MDD patients and covarying for antidepressant use, comorbidity, melancholic and atypical MDD symptoms, sociodemographics (age, sex, education), and scan location likewise did not affect the documented UNC and CIN effects (UNC: $\beta = -0.40$, $P < 0.05$; CIN: $\beta = -0.57$, $P < 0.05$).

6.2.4. AD specifier vs. comorbid anxiety disorder

Post-hoc analyses additionally assessed whether the presence of the AD specifier vs. current comorbid anxiety disorders may relate to distinct or overlapping WM effects. To this end, the categorical TBSS analyses were rerun, but instead of using the AD specifier for MDD groupings, the presence of comorbid anxiety disorders was now used to form MDD groups. MDD patients with comorbidity (N = 21), without comorbidity (N = 28), and HC participants (N = 39) were subsequently compared on WM integrity, using exactly the same analytical approach as the primary categorical TBSS analyses. The analyses, however, revealed no significant effects within the UNC, CIN, ATR, or any other WM tracts (P's > 0.20, *TFCE* & *FWE* corrected). This suggests a weak overlap between WM correlates of the AD specifier and comorbid anxiety disorders among our MDD patients, cautiously hinting that the findings are specific to MDD/AD+.

6.2.5. Receiver-operating characteristics (ROC)

To explore the sensitivity and specificity of the between-groups ATR effect in classifying MDD/AD+ patients versus MDD/AD- and HC participants, ROC analyses (SPSS, Version 25, IBM Corp., Armonk, N.Y., USA) were conducted. Similar to prior work (Ellard et al., 2018), mean FA values from ATR regions of significant effect were entered as the test variable, with diagnostic group entered as the state variable, assuming a nonparametric distribution. Resulting cutoff scores representing the greatest balance between highest sensitivity and specificity (i.e., Youden Index) were used to calculate sample-based sensitivity/specificity proportions. Microstructural integrity within the ATR effects site was moderately successful in classifying MDD/AD+ patients versus MDD/AD- and HC participants (*AUC* = 0.83, *SE* = 0.05, $P < 0.001$, *CI* = 0.74—0.92), with 90% sensitivity, 73% specificity, and 77% accuracy (see Fig. 5). When looking at the two patient groups alone, ATR microstructural integrity was still fairly successful in discriminating MDD/AD+ from MDD/AD- patients (*AUC* = 0.78, *SE* = 0.07, P = 0.001, *CI* = 0.65—0.91), with 90% sensitivity, 66% specificity, and 75% accuracy (see Fig. 5).

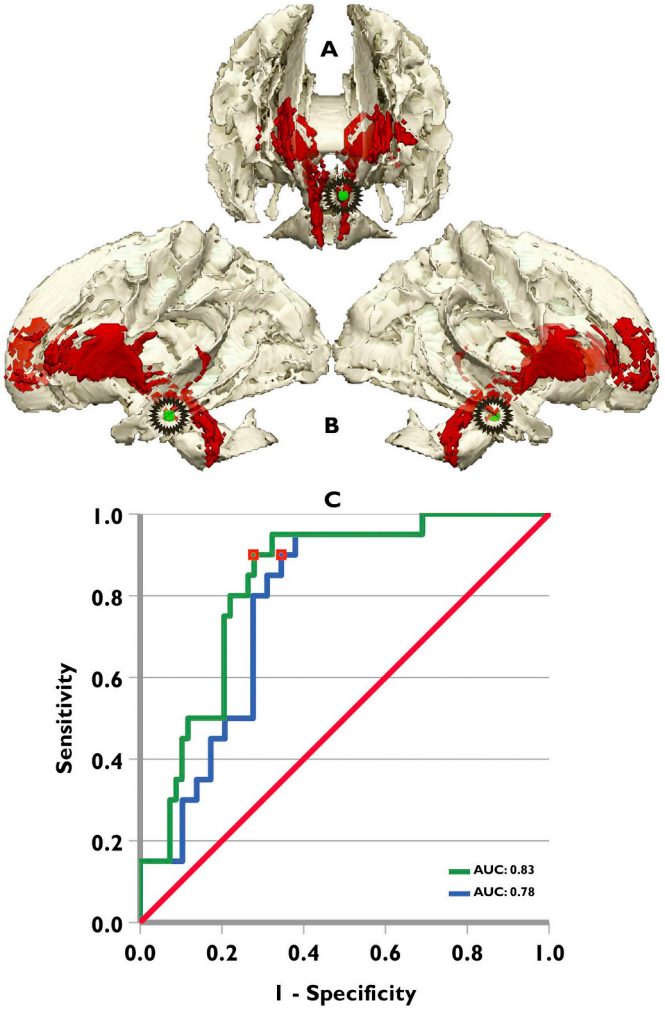

Fig. 5. Receiver-operating characteristics (ROC) analysis. To explore the sensitivity and specificity of the between-groups ATR effect in classifying MDD/AD + patients versus MDD/AD- and HC participants, ROC analyses were conducted. Microstructural integrity (i.e., mean FA) within the ATR effects site (A & B) was moderately successful in classifying MDD/AD + patients versus MDD/AD- and HC participants ($AUC = 0.83$, $SE = 0.05$, $P < 0.001$, $CI = 0.74—0.92$), with 90% sensitivity, 73% specificity, and 77% accuracy (C, green ROC curve). When looking at the two patient groups alone, ATR microstructural integrity was still fairly successful in discriminating MDD/AD + from MDD/AD- patients ($AUC = 0.78$, $SE = 0.07$, $P = 0.001$, $CI = 0.65—0.91$), with 90% sensitivity, 66% specificity, and 75% accuracy (C, blue ROC curve). Red squares represent the point of greatest balance between maximum sensitivity and specificity (i.e., Youden Index). Brain images in A & B provide a representative view of the WM skeleton (beige/grey) and the ATR tract (red), along with the ATR subregion (green) that exhibited significantly reduced FA in MDD/AD + patients relative to MDD/AD- and HC participants, respectively. Black edged circles mark the effect site for better visibility. MDD/AD + = Major Depressive Disorder *with* Anxious Distress; MDD/AD- = Major Depressive Disorder *without* Anxious Distress; HC = Healthy Controls; ATR = Anterior Thalamic Radiation; WM = White Matter; FA = Fractional Anisotropy. (For interpretation of the references to colour in this figure legend, the reader is referred to the web version of this article.)

7. Discussion

The current study uniquely probed whether MDD/AD +, as informed by DSM-5, relates to distinct perturbations in WM architecture. Whereas categorical analyses revealed diminished ATR integrity in MDD/AD + patients relative to MDD/AD- and HC participants, dimensional analyses within MDD patients linked elevated AD specifier scores to diminished integrity of the UNC and CIN tracts. These effects were not confounded by key clinical and sociodemographic factors, with altered ATR integrity moreover successfully classifying MDD/AD + patients from MDD/AD- and HC participants. These novel findings collectively link MDD/AD + to distinct WM anomalies in frontolimbic tracts important to adaptive emotional functioning. The findings may thus provide relevant, yet preliminary, clues on MDD/AD + pathophysiology by highlighting WM microstructural changes as a putative pathomechanism.

7.1. Categorical approach

Our categorical *between-groups* analysis revealed diminished FA values in the ATR among MDD/AD + patients, which were coupled with elevated A.Dif, R.Dif, M.Dif levels, possibly suggestive of abnormal fiber bundle coherence (i.e. elevated A.Dif), demyelination (i.e. elevated R.Dif), and diminished cellularity (i.e. elevated M.Dif), (Alexander et al., 2007). This change in ATR microstructure moreover successfully classified MDD/AD + patients from MDD/AD- and HC participants (90% sensitivity | 73% specificity | 77% accuracy). Several DTI studies link perturbed ATR microstructure to MDD pathophysiology, as well as abnormal fear processing and anxiety (Albaugh et al., 2017a; Coenen et al., 2012; Deng et al., 2018; Jenkins et al., 2016; Lai and Wu, 2014; Liu et al., 2016; Wang et al., 2016; Westlye et al., 2011). Most of these studies converge on lower FA values in the ATR among individuals with depressive and/or anxious symptomologies (Albaugh et al., 2017a; Deng et al., 2018; Lai and Wu, 2014; Liu et al., 2016; Westlye et al., 2011), echoing the findings presented here.

The ATR is a frontolimbic tract that links various thalamic subregions to lateral and medial PFC territories (Bracht et al., 2015; Cho et al., 2015), and is deemed relevant to the expression of emotions (Coenen et al., 2012; Deng et al., 2018; Spalletta et al., 2013). In fact, abnormalities in the ATR have been tentatively theorized to upset the dynamic equilibrium between positive and negative affective states, potentially rendering an individual vulnerable to mood dysregulation (Coenen et al., 2012). The ATR is furthermore argued to play an important role in physiological distress and arousal (Coenen et al., 2012; Kirouac, 2015), as it connects PFC and thalamic regions with central autonomic structures such as the brainstem/substantia nigra territory (Cho et al., 2015). Interestingly, this is also where we observed alterations in ATR microstructure among MDD/AD + patients (Fig. 2). The brainstem/substantia nigra territory was also implicated in a prior DTI study on MDD with anxiety features (Blood et al., 2010), though this concerned more the grey matter segments of this territory rather than its ATR section, wherein the FA was intriguingly elevated. While differences in methodology (TBSS vs. Voxelwise DTI) and effect site (white vs. grey matter) may explain the opposing FA effects in this region, they collectively converge on the relevance of the brainstem/substantia nigra territory to MDD with anxiety features. Taken as a whole, the ATR effect documented here might thus provide preliminary insights into a putative substrate for MDD/AD +, which ostensibly carries relevance for emotional homeostasis on the cognitive, behavioral, and physiological level. Our classification analyses seem to partly support this tentative notion by additionally showing the sensitivity and specificity of these ATR effects. The findings, however, warrant cautious interpretation, further investigation, and future replication, given their exploratory nature and our incomplete understanding of ATR contributions to (mal)adaptive emotional function.

7.2. Dimensional approach

Our *within-patients* dimensional analysis additionally revealed that higher AD scores related to lower FA values in the OFC section of the UNC and ventral ACC segment of the CIN. Examination of diffusivity measures suggested these FA changes to be largely driven by decreased A.Dif, increased R.Dif, and preserved M.Dif, thus putatively linking AD

symptoms in MDD to demyelination (i.e., increased R.Dif) and axonal disintegrity (i.e., decreased A.Dif) within the UNC and CIN (Alexander et al., 2007). Various studies implicate abnormal UNC and CIN microstructure in the pathophysiology of depression and anxiety, with generally lower FA values being found within these tracts in depressed and/or anxious individuals (Bhatia et al., 2018; Bracht et al., 2015; Cullen et al., 2010), thus echoing the findings presented here. The UNC mainly connects the amygdalar/hippocampal complexes to ventral frontal territories (e.g., OFC) (Von Der Heide et al., 2013), while CIN bundles allow for more widely-distributed interconnections by linking prefrontal, cingulate, parietal and medial temporal territories (Bubb et al., 2018; Wu et al., 2016). Their combined connectivity profiles are therefore deemed crucial to adaptive frontolimbic communications that serve to support various aspects of human emotional behavior (Bhatia et al., 2018; Bracht et al., 2015; Cullen et al., 2010; Keedwell et al., 2012; Keedwell and Linden, 2013; Sexton et al., 2009).

Alterations in UNC and CIN microstructure documented here thus seem to reverberate the centrality of these WM tracts to the frontolimbic system dysfunction that is commonly hypothesized in affective psychopathologies, and in specific MDD/AD+ (Gaspersz et al., 2017b; Gaspersz et al., 2017; Gaspersz et al., 2018; Phillips et al., 2015). The location of WM alterations we find for the UNC and CIN (OFC and ventral ACC region, respectively), however, seems more suggestive of perturbations in the ventral subsegment of this frontolimbic system (Phillips et al., 2015; Phillips et al., 2008). This ventral frontolimbic subsystem comprises the amygdala, subgenual/ventral ACC, ventrolateral PFC, and OFC, and is among other things, heavily involved in encoding the emotional significance of a stimulus and producing an affective response to it (Phillips et al., 2015; Phillips et al., 2008; Stein et al., 2007). As the OFC and ventral ACC crucially link subcortically-generated information with higher-order cortical computations, and vice versa, (Etkin et al., 2011; Fatahi et al., 2018; Phillips et al., 2015; Zhu et al., 2011), our findings may point to aberrant frontolimbic transmission of emotional/affective information, which speculatively could impede how emotions are perceived, processed, and controlled (Gaspersz et al., 2018; Phillips et al., 2015; Phillips et al., 2008). The fact that the ventral frontal segments of the UNC and CIN are prime target sites for deep-brain stimulation in treatment-resistant depression seems to further highlight their importance to adaptive emotional function (Choi et al., 2015; Howell et al., 2019; Lujan et al., 2012; Noecker et al., 2018; Riva-Posse et al., 2018; Riva-Posse et al., 2014). The ventral/subgenual ACC section of the CIN, however, seems of particular relevance in this context, for its stimulation tends to produce far more superior and enduring antidepressant effects than stimulating the “confluence point” of ventrofrontal UNC and CIN regions (Howell et al., 2019). While the data presented here highlight the importance of the UNC and CIN to (mal)adaptive emotional function, future studies are warranted for further exploration and validation, given the intricate modulation of human emotions by frontolimbic circuits.

7.3. Categorical versus dimensional approach

Due to the prevalence of comorbidity and multi-sourced etiologies, psychopathological research benefits from an integrative approach combining categorical and dimensional measures of psychiatric entities (Fuchs, 2010; Fuchs and Pallagrosi, 2018; Hudziak et al., 2007). Though the categorical approach at first sight may seem more appealing and clinically relevant, especially in the context of DSM, it may not fully pick up the inter-subject variability that is unmistakably present among MDD patients (Fuchs, 2010; Hudziak et al., 2007). Hence, many scholars suggest the complementary application of categorical and dimensional analyses in psychiatry (Fuchs and Pallagrosi, 2018), even when examining a specific subgroup/subtype based on a predefined specifier (Dillon et al., 2018; Hudziak et al., 2007). Consonant with this notion, the current study innovatively probed the impact of the DSM-5 Anxious Distress specifier for MDD on WM architecture both categorically and dimensionally. While both approaches interestingly revealed the same trend/effect as a function of Anxious Distress symptoms (i.e., reduced WM integrity), the location of WM changes differed between approaches (categorical = ATR tract; dimensional = UNC & CIN tracts). This could speculatively suggest that ATR microstructure might be more relevant for differentiating MDD/AD+ from other MDD subtypes and healthy controls, a notion partly supported by our classification analyses, whereas alterations in UNC and CIN seem more indicative of MDD/AD+ severity. Future research on MDD subtyping should further explore and validate these tentative interpretations, ideally employing both categorical and dimensional approaches and comparing different subtypes simultaneously, in search for commonalities and unique subtype characteristics.

7.4. Study limitations and strengths

The cross-sectional nature of this study does not allow for firm conclusions regarding causality. Hence, we cannot ascertain whether microstructural alterations reported in this study preceded or followed the onset of MDD/AD+. The sample size is moreover relatively small, though fairly similar to prior structural MRI work on DSM-informed MDD subtypes (Bracht et al., 2014; Dillon et al., 2018; Ota et al., 2015; Zhao et al., 2017). Longitudinal research in larger samples with a wide age range, and DTI studies of individuals at risk for affective disorders, could tackle these limitations. Although DTI is a useful tool for characterizing WM microstructure (Lim and Helpern, 2002), it only provides a proxy for actual WM integrity (Beaulieu, 2002; Jones et al., 2013; Soares et al., 2013). Caution is thus warranted in interpreting FA changes as actual changes or differences in WM “integrity”. While our post-hoc analyses revealed no significant impact of key clinical and sociodemographic confounds on documented WM effects, cautious interpretation of the findings is nevertheless warranted, given the difficulties to fully tease out/eliminate confounders (especially in smaller samples). The same cautiousness also applies to our classification analysis/finding, which necessitates replication and further exploration in preferably larger studies to reaffirm its accuracy.

Notwithstanding these limitations, our findings do merit attention as the first evidence for fairly specific and discriminant WM anomalies in MDD patients that meet the DSM-5 informed Anxious Distress specifier, which is novel within the field of MDD subtyping. Previous DTI studies have tried to address this issue, though fairly indirectly by either using a AD specifier not conforming to DSM-5 criteria or comparing MDD patients with vs. without comorbid anxiety on WM integrity (e.g., Delaparte et al., 2017; Xia et al., 2018). However, MDD with a comorbid anxiety disorder captures a partially different group of patients than MDD/AD+ (Gaspersz et al., 2017a; Rosellini et al., 2018), as evidenced by the poor overlap between the presence of the AD specifier and comorbid anxiety disorders among MDD patients (Gaspersz et al., 2017a). The current study corroborates this premise, as MDD/AD+ and MDD/AD- patients did not differ in terms of comorbid anxiety diagnoses (see Table 1), while our post-hoc analyses found no overlap between WM correlates of the AD specifier and comorbid anxiety disorders in MDD patients. This may cautiously hint that the findings documented here are specific to MDD/AD+, and plausibly allow deeper insights into MDD/AD+ pathophysiology. The fact that melancholic and atypical MDD symptoms did not affect any of the WM effects documented here seems to further corroborate their specificity to AD symptoms. The conjoint categorical and dimensional examination of AD-specific effects on WM, matching of groups on sociodemographics, and correction for key confounds to the best of our abilities, tend to moreover increase the reliability of the findings.

8. Conclusions

The data presented here collectively link MDD/AD+ to distinct WM anomalies in frontolimbic tracts important to adaptive emotional

functioning. The findings seem to provide relevant, yet preliminary, clues on MDD/AD+ pathophysiology by highlighting WM microstructural changes as a putative pathomechanism. For a deeper understanding of WM architecture in MDD/AD+, it would be important to examine whether WM alterations predict susceptibility, chronicity and treatment response in this specific class of MDD patients. Ideally, these future studies should be longitudinal and employ multimodal imaging, in which structural and functional connectivity of relevant frontolimbic tracts are simultaneously investigated.

Conflict of interests

The authors report no conflict of interest.

Contributors

Gijs Jurjen Heij and Moji Aghajani contributed to the conceptualization, design, methodology, and data analysis of this paper. All authors contributed to the writing of the paper.

Financial disclosure

Dr. Brenda Penninx has received research funding from Jansen Research & Development, LLC, and Boehringer Ingelheim.

Ethical statement

Our study was conducted in accordance with the declaration of Helsinki and approved by the medical ethics committee of the VU University Medical Center. We declare that written informed consent was obtained from all participants. The authors furthermore declare no conflict of interest.

Acknowledgements

The infrastructure for the NESDA study (www.nesda.nl) is funded through the Geestkracht program of the Netherlands Organization for Health Research and Development (ZonMw, grant number 10-000-1002) and through participating universities (VU University Medical Centre, Leiden University Medical Centre, University Medical Centre Groningen). M.J.van.Tol was supported by a VENI grant from the Netherlands Organization for Scientific Research (NWO grant number: 016.156.077).

References

Aghajani, M., Veer, I.M., van Lang, N.D., Meens, P.H., van den Bulk, B.G., Rombouts, S.A., Vermeiren, R.R., van der Wee, N.J., 2014. Altered white-matter architecture in treatment-naive adolescents with clinical depression. Psychol. Med. 44 (11), 2287–2298.

Albaugh, M.D., Ducharme, S., Karama, S., Watts, R., Lewis, J.D., Orr, C., Nguyen, T.V., McKinstry, R.C., Botteron, K.N., Evans, A.C., Hudziak, J.J., Brain Development Cooperative, G., 2017a. Anxious/depressed symptoms are related to microstructural maturation of white matter in typically developing youths. Dev. Psychopathol. 29 (3), 751–758.

Albaugh, M.D., Ducharme, S., Karama, S., Watts, R., Lewis, J.D., Orr, C., Nguyen, T.V., Mckinstry, R.C., Botteron, K.N., Evans, A.C., Hudziak, J.J., Grp, B.D.C., 2017b. Anxious/depressed symptoms are related to microstructural maturation of white matter in typically developing youths. Dev. Psychopathol. 29 (3), 751–758.

Alexander, A.L., Lee, J.E., Lazar, M., Field, A.S., 2007. Diffusion tensor imaging of the brain. Neurotherapeutics 4 (3), 316–329.

Alves, G.S., Oertel Knochel, V., Knochel, C., Carvalho, A.F., Pantel, J., Engelhardt, E., Laks, J., 2015. Integrating retrogenesis theory to Alzheimer's disease pathology: insight from DTI-TBSS investigation of the white matter microstructural integrity. Biomed. Res. Int. 2015, 291658.

Andersson, J.L.R., Sotiropoulos, S.N., 2016. An integrated approach to correction for off-resonance effects and subject movement in diffusion MR imaging. Neuroimage 125, 1063–1078.

Andersson, J.L.R., Skare, S., Ashburner, J., 2003. How to correct susceptibility distortions in spin-echo echo-planar images: application to diffusion tensor imaging. Neuroimage 20 (2), 870–888.

Andersson, J.L.R., Graham, M.S., Zsoldos, E., Sotiropoulos, S.N., 2016. Incorporating outlier detection and replacement into a non-parametric framework for movement and distortion correction of diffusion MR images. Neuroimage 141, 556–572.

Andrews, G., Peters, L., 1998. The psychometric properties of the composite international diagnostic interview. Soc. Psychiatry Psychiatr. Epidemiol. 33 (2), 80–88.

APA, 2013. Diagnostic and Statistical Manual of Mental Disorders, 5th ed. American Psychiatric Publishing, Washington, DC.

Beaulieu, C., 2002. The basis of anisotropic water diffusion in the nervous system - a technical review. NMR Biomed. 15 (7–8), 435–455.

Beck, A.T., Epstein, N., Brown, G., Steer, R.A., 1988. An inventory for measuring clinical anxiety: psychometric properties. J. Consult. Clin. Psychol. 56 (6), 893–897.

Behrens, T.E., Woolrich, M.W., Jenkinson, M., Johansen-Berg, H., Nunes, R.G., Clare, S., Matthews, P.M., Brady, J.M., Smith, S.M., 2003. Characterization and propagation of uncertainty in diffusion-weighted MR imaging. Magn. Reson. Med. 50 (5), 1077–1088.

Belmaker, R.H., Agam, G., 2008. Major depressive disorder. N. Engl. J. Med. 358 (1), 55–68.

Bhatia, K.D., Henderson, L.A., Hsu, E., Yim, M., 2018. Reduced integrity of the uncinate fasciculus and cingulum in depression: a stem-by-stem analysis. J. Affect. Disord. 235, 220–228.

Blood, A.J., Iosifescu, D.V., Makris, N., Perlis, R.H., Kennedy, D.N., Dougherty, D.D., Kim, B.W., Lee, M.J., Wu, S., Lee, S., Calhoun, J., Hodge, S.M., Fava, M., Rosen, B.R., Smoller, J.W., Gasic, G.P., Breiter, H.C., Phenotype Genotype Project on, A., Mood, D, 2010. Microstructural abnormalities in subcortical reward circuitry of subjects with major depressive disorder. PLoS One 5 (11), e13945.

Bracht, T., Horn, H., Strik, W., Federspiel, A., Schnell, S., Hofle, O., Stegmayer, K., Wiest, R., Dierks, T., Muller, T.J., Walther, S., 2014. White matter microstructure alterations of the medial forebrain bundle in melancholic depression. J. Affect. Disord. 155, 186–193.

Bracht, T., Linden, D., Keedwell, P., 2015. A review of white matter microstructure alterations of pathways of the reward circuit in depression. J. Affect. Disord. 187, 45–53.

Bubb, E.J., Metzler-Baddeley, C., Aggleton, J.P., 2018. The cingulum bundle: anatomy, function, and dysfunction. Neurosci. Biobehav. Rev. 92, 104–127.

Budde, M.D., Xie, M., Cross, A.H., Song, S.K., 2009. Axial diffusivity is the primary correlate of axonal injury in the experimental autoimmune encephalomyelitis spinal cord: a quantitative Pixelwise analysis. J. Neurosci. 29 (9), 2805–2813.

Caetano, S.C., Fonseca, M., Hatch, J.P., Olvera, R.L., Nicoletti, M., Hunter, K., Lafer, B., Pliszka, S.R., Soares, J.C., 2007. Medial temporal lobe abnormalities in pediatric unipolar depression. Neurosci. Lett. 427 (3), 142–147.

Canu, E., Kostic, M., Agosta, F., Munjiza, A., Ferraro, P.M., Pesic, D., Copetti, M., Peljto, A., Lecic Tosevski, D., Filippi, M., 2015. Brain structural abnormalities in patients with major depression with or without generalized anxiety disorder comorbidity. J. Neurol. 262 (5), 1255–1265.

Cho, Z.H., Law, M., Chi, J.G., Choi, S.H., Park, S.Y., Kammen, A., Park, C.W., Oh, S.H., Kim, Y.B., 2015. An anatomic review of thalamolimbic fiber tractography: ultra-high resolution direct visualization of thalamolimbic fibers anterior thalamic radiation, superolateral and inferomedial medial forebrain bundles, and newly identified septum pellucidum tract. World Neurosurg 83 (1), 54–61 (e32).

Choi, K.S., Holtzheimer, P.E., Franco, A.R., Kelley, M.E., Dunlop, B.W., Hu, X.P., Mayberg, H.S., 2014. Reconciling variable findings of white matter integrity in major depressive disorder. Neuropsychopharmacology 39 (6), 1332–1339.

Choi, K.S., Riva-Posse, P., Gross, R.E., Mayberg, H.S., 2015. Mapping the "depression switch" during intraoperative testing of subcallosal cingulate deep Brain stimulation. JAMA Neurol. 72 (11), 1252–1260.

Coenen, V.A., Panksepp, J., Hurwitz, T.A., Urbach, H., Madler, B., 2012. Human medial forebrain bundle (MFB) and anterior thalamic radiation (ATR): imaging of two major subcortical pathways and the dynamic balance of opposite affects in understanding depression. J. Neuropsychiatr. Clin. Neurosci. 24 (2), 223–236.

Cohen, M.X., Elger, C.E., Weber, B., 2008. Amygdala tractography predicts functional connectivity and learning during feedback-guided decision-making. Neuroimage 39 (3), 1396–1407.

Concha, L., Gross, D.W., Beaulieu, C., 2005. Diffusion tensor tractography of the limbic system. AJNR Am. J. Neuroradiol. 26 (9), 2267–2274.

Cullen, K.R., Klimes-Dougan, B., Muetzel, R., Mueller, B.A., Camchong, J., Houri, A., Kurma, S., Lim, K.O., 2010. Altered white matter microstructure in adolescents with major depression: a preliminary study. J. Am. Acad. Child Adolesc. Psychiatry 49 (2), 173–183 e171.

Cullen, K.R., Westlund, M.K., Klimes-Dougan, B., Mueller, B.A., Houri, A., Eberly, L.E., Lim, K.O., 2014. Abnormal amygdala resting-state functional connectivity in adolescent depression. JAMA Psychiatr. 10, 1138–1147.

Delaparte, L., Yeh, F.C., Adams, P., Malchow, A., Trivedi, M.H., Oquendo, M.A., Deckersbach, T., Ogden, T., Pizzagalli, D.A., Fava, M., Cooper, C., McInnis, M., Kurian, B.T., Weissman, M.M., McGrath, P.J., Klein, D.N., Parsey, R.V., DeLorenzo, C., 2017. A comparison of structural connectivity in anxious depression versus non-anxious depression. J. Psychiatr. Res. 89, 38–47.

Deng, F., Wang, Y., Huang, H., Niu, M., Zhong, S., Zhao, L., Qi, Z., Wu, X., Sun, Y., Niu, C., He, Y., Huang, L., Huang, R., 2018. Abnormal segments of right uncinate fasciculus and left anterior thalamic radiation in major and bipolar depression. Prog. Neuropsychopharmacol. Bol. Psychiatr. 81, 340–349.

Dillon, D.G., Gonenc, A., Belleau, E., Pizzagalli, D.A., 2018. Depression is associated with dimensional and categorical effects on white matter pathways. Depress. Anxiety 35 (5), 440–447.

Disner, S.G., Beevers, C.G., Haigh, E.A., Beck, A.T., 2011. Neural mechanisms of the cognitive model of depression. Nat. Rev. Neurosci. 12 (8), 467–477.

Eickhoff, S.B., Paus, T., Caspers, S., Grosbras, M.H., Evans, A.C., Zilles, K., Amunts, K.,

2007. Assignment of functional activations to probabilistic cytoarchitectonic areas revisited. Neuroimage 36 (3), 511–521.
Ellard, K.K., Zimmerman, J.P., Kaur, N., Van Dijk, K.R.A., Roffman, J.L., Nierenberg, A.A., Dougherty, D.D., Deckersbach, T., Camprodon, J.A., 2018. Functional connectivity between anterior insula and key nodes of frontoparietal executive control and salience networks distinguish bipolar depression from unipolar depression and healthy control subjects. Biol. Psychiatr. Cogn. Neurosci. Neuroimaging 3 (5), 473–484.
Etkin, A., Egner, T., Kalisch, R., 2011. Emotional processing in anterior cingulate and medial prefrontal cortex. Trends Cogn. Sci. 15 (2), 85–93.
Fatahi, Z., Haghparast, A., Khani, A., Kermani, M., 2018. Functional connectivity between anterior cingulate cortex and orbitofrontal cortex during value-based decision making. Neurobiol. Learn. Mem. 147, 74–78.
Fuchs, T., 2010. Subjectivity and intersubjectivity in psychiatric diagnosis. Psychopathology 43 (4), 268–274.
Fuchs, T., Pallagrosi, M., 2018. Phenomenology of temporality and dimensional psychopathology. In: Biondi, M., Pasquini, M., Picardi, A. (Eds.), Dimensional Psychopathology. Springer, Cham, pp. 287–300.
Gaspersz, R., Lamers, F., Wittenberg, G., Beekman, A.T.F., van Hemert, A.M., Schoevers, R.A., Penninx, B., 2017. The role of anxious distress in immune dysregulation in patients with major depressive disorder. Transl. Psychiatry 7 (12), 1268.
Gaspersz, R., Lamers, F., Kent, J.M., Beekman, A.T., Smit, J.H., van Hemert, A.M., Schoevers, R.A., Penninx, B.W.J.H., 2017a. Longitudinal predictive validity of the DSM-5 anxious distress specifier for clinical outcomes in a large cohort of patients with major depressive disorder. J. Clin. Psychiatr. 78 (2), 207–213.
Gaspersz, R., Lamers, F., Kent, J.M., Beekman, A.T.F., Smit, J.H., van Hemert, A.M., Schoevers, R.A., Penninx, B.W.J.H., 2017b. Anxious distress predicts subsequent treatment outcome and side effects in depressed patients starting antidepressant treatment. J. Psychiatr. Res. 84, 41–48.
Gaspersz, R., Nawijn, L., Lamers, F., Penninx, B.W.J.H., 2018. Patients with anxious depression: overview of prevalence, pathophysiology and impact on course and treatment outcome. Curr. Opin. Psychiatr. 31 (1), 17–25.
Horsfield, M.A., Jones, D.K., 2002. Applications of diffusion-weighted and diffusion tensor MRI to white matter diseases - a review. NMR Biomed. 15 (7–8), 570–577.
Howell, B., Choi, K.S., Gunalan, K., Rajendra, J., Mayberg, H.S., McIntyre, C.C., 2019. Quantifying the axonal pathways directly stimulated in therapeutic subcallosal cingulate deep brain stimulation. Hum. Brain Mapp. 40 (3), 889–903.
Hudziak, J.J., Achenbach, T.M., Althoff, R.R., Pine, D.S., 2007. A dimensional approach to developmental psychopathology. Int. J. Methods Psychiatr. Res. 16 (Suppl. 1), S16–S23.
Ionescu, D.F., Niciu, M.J., Mathews, D.C., Richards, E.M., Zarate Jr., C.A., 2013. Neurobiology of anxious depression: a review. Depress. Anxiety 30 (4), 374–385.
Jenkins, L.M., Barba, A., Campbell, M., Lamar, M., Shankman, S.A., Leow, A.D., Ajilore, O., Langenecker, S.A., 2016. Shared white matter alterations across emotional disorders: a voxel-based meta-analysis of fractional anisotropy. Neuroimage Clin. 12, 1022–1034.
Jiang, J., Zhao, Y.J., Hu, X.Y., Du, M.Y., Chen, Z.Q., Wu, M., Li, K.M., Zhu, H.Y., Kumar, P., Gong, Q.Y., 2017. Microstructural brain abnormalities in medication-free patients with major depressive disorder: a systematic review and meta-analysis of diffusion tensor imaging. J. Psychiatry Neurosci. 42 (3), 150–163.
Jones, D.K., Knosche, T.R., Turner, R., 2013. White matter integrity, fiber count, and other fallacies: the do's and don'ts of diffusion MRI. Neuroimage 73, 239–254.
Keedwell, P.A., Linden, D.E., 2013. Integrative neuroimaging in mood disorders. Curr. Opin. Psychiatr. 26 (1), 27–32.
Keedwell, P.A., Chapman, R., Christiansen, K., Richardson, H., Evans, J., Jones, D.K., 2012. Cingulum white matter in young women at risk of depression: the effect of family history and anhedonia. Biol. Psychiatry 72 (4), 296–302.
Kessler, R.C., Sampson, N.A., Berglund, P., Gruber, M.J., Al-Hamzawi, A., Andrade, L., Bunting, B., Demyttenaere, K., Florescu, S., de Girolamo, G., Gureje, O., He, Y., Hu, C., Huang, Y., Karam, E., Kovess-Masfety, V., Lee, S., Levinson, D., Medina Mora, M.E., Moskalewicz, J., Nakamura, Y., Navarro-Mateu, F., Browne, M.A., Piazza, M., Posada-Villa, J., Slade, T., Ten Have, M., Torres, Y., Vilagut, G., Xavier, M., Zarkov, Z., Shahly, V., Wilcox, M.A., 2015. Anxious and non-anxious major depressive disorder in the World Health Organization world mental health surveys. Epidemiol. Psychiatr. Sci. 24 (3), 210–226.
Khan, A.Y., Carrithers, J., Preskorn, S.H., Lear, R., Wisniewski, S.R., John Rush, A., Stegman, D., Kelley, C., Kreiner, K., Nierenberg, A.A., Fava, M., 2006. Clinical and demographic factors associated with DSM-IV melancholic depression. Ann. Clin. Psychiatry 18 (2), 91–98.
Kirouac, G.J., 2015. Placing the paraventricular nucleus of the thalamus within the brain circuits that control behavior. Neurosci. Biobehav. Rev. 56, 315–329.
Kochunov, P., Thompson, P.M., Lancaster, J.L., Bartzokis, G., Smith, S., Coyle, T., Royall, D.R., Laird, A., Fox, P.T., 2007. Relationship between white matter fractional anisotropy and other indices of cerebral health in normal aging: tract-based spatial statistics study of aging. Neuroimage 35 (2), 478–487.
Lai, C.H., Wu, Y.T., 2014. Alterations in white matter micro-integrity of the superior longitudinal fasciculus and anterior thalamic radiation of young adult patients with depression. Psychol. Med. 44 (13), 2825–2832.
Lener, M.S., Iosifescu, D.V., 2015. In pursuit of neuroimaging biomarkers to guide treatment selection in major depressive disorder: a review of the literature. Ann. N. Y. Acad. Sci. 1344, 50–65.
LeWinn, K.Z., Connolly, C.G., Wu, J., Drahos, M., Hoeft, F., Ho, T.C., Simmons, A.N., Yang, T.T., 2014. White matter correlates of adolescent depression: structural evidence for frontolimbic disconnectivity. J. Am. Acad. Child Adolesc. Psychiatry 53 (8), 899–909 (909 e891–897).
Liao, Y., Huang, X., Wu, Q., Yang, C., Kuang, W., Du, M., Lui, S., Yue, Q., Chan, R.C., Kemp, G.J., Gong, Q., 2013. Is depression a disconnection syndrome? Meta-analysis of diffusion tensor imaging studies in patients with MDD. J. Psychiatry Neurosci. 38 (1), 49–56.
Lim, K.O., Helpern, J.A., 2002. Neuropsychiatric applications of DTI - a review. NMR Biomed. 15 (7–8), 587–593.
Liu, X., Watanabe, K., Kakeda, S., Yoshimura, R., Abe, O., Ide, S., Hayashi, K., Katsuki, A., Umene-Nakano, W., Watanabe, R., Ueda, I., Nakamura, J., Korogi, Y., 2016. Relationship between white matter integrity and serum cortisol levels in drug-naive patients with major depressive disorder: diffusion tensor imaging study using tract-based spatial statistics. Br. J. Psychiatry 208 (6), 585–590.
Lujan, J.L., Chaturvedi, A., Malone, D.A., Rezai, A.R., Machado, A.G., McIntyre, C.C., 2012. Axonal pathways linked to therapeutic and nontherapeutic outcomes during psychiatric deep brain stimulation. Hum. Brain Mapp. 33 (4), 958–968.
Mayberg, H.S., 2003. Modulating dysfunctional limbic-cortical circuits in depression: towards development of brain-based algorithms for diagnosis and optimised treatment. Br. Med. Bull. 65, 193–207.
Mori, S., Wakana, S., Nagae-Poetscher, L.M., van Zijl, P.C.M., 2005. MRI Atlas of Human White Matter. Elsevier, Amsterdam, The Netherlands.
Noecker, A.M., Choi, K.S., Riva-Posse, P., Gross, R.E., Mayberg, H.S., McIntyre, C.C., 2018. StimVision software: examples and applications in subcallosal cingulate deep brain stimulation for depression. Neuromodulation 21 (2), 191–196.
Novick, J.S., Stewart, J.W., Wisniewski, S.R., Cook, I.A., Manev, R., Nierenberg, A.A., Rosenbaum, J.F., Shores-Wilson, K., Balasubramani, G.K., Biggs, M.M., Zisook, S., Rush, A.J., investigators, S.D., 2005. Clinical and demographic features of atypical depression in outpatients with major depressive disorder: preliminary findings from STAR*D. J. Clin. Psychiatr. 66 (8), 1002–1011.
Olson, I.R., Von Der Heide, R.J., Alm, K.H., Vyas, G., 2015. Development of the uncinate fasciculus: implications for theory and developmental disorders. Dev. Cogn. Neurosci. 14, 50–61.
Ota, M., Noda, T., Sato, N., Hattori, K., Hori, H., Sasayama, D., Teraishi, T., Nagashima, A., Obu, S., Higuchi, T., Kunugi, H., 2015. White matter abnormalities in major depressive disorder with melancholic and atypical features: a diffusion tensor imaging study. Psychiatry Clin. Neurosci. 69 (6), 360–368.
Penninx, B.W.J.H., Beekman, A.T., Smit, J.H., Zitman, F.G., Nolen, W.A., Spinhoven, P., Cuijpers, P., De Jong, P.J., Van Marwijk, H.W., Assendelft, W.J., Van Der Meer, K., Verhaak, P., Wensing, M., De Graaf, R., Hoogendijk, W.J., Ormel, J., Van Dyck, R., Consortium, N.R., 2008. The Netherlands study of depression and anxiety (NESDA): rationale, objectives and methods. Int. J. Methods Psychiatr. Res. 17 (3), 121–140.
Pessoa, L., 2008. On the relationship between emotion and cognition. Nat. Rev. Neurosci. 9 (2), 148–158.
Petrides, M., Pandya, D.N., 2002. Comparative cytoarchitectonic analysis of the human and the macaque ventrolateral prefrontal cortex and corticocortical connection patterns in the monkey. Eur. J. Neurosci. 16 (2), 291–310.
Phillips, M.L., Drevets, W.C., Rauch, S.L., Lane, R., 2003. Neurobiology of emotion perception II: implications for major psychiatric disorders. Biol. Psychiatry 54 (5), 515–528.
Phillips, M., Ladouceur, C., Drevets, W., 2008. A neural model of voluntary and automatic emotion regulation: implications for understanding the pathophysiology and neurodevelopment of bipolar disorder. Mol. Psychiatry 13 (9), 833–857.
Phillips, M.L., Chase, H.W., Sheline, Y.I., Etkin, A., Almeida, J.R., Deckersbach, T., Trivedi, M.H., 2015. Identifying predictors, moderators, and mediators of antidepressant response in major depressive disorder: neuroimaging approaches. A. J. Psychiatr. 172 (2), 124–138.
Potvin, O., Catheline, G., Bernard, C., Meillon, C., Bergua, V., Allard, M., Dartigues, J.F., Chauveau, N., Celsis, P., Amieva, H., 2015. Gray matter characteristics associated with trait anxiety in older adults are moderated by depression. Int. Psychogeriatr. 27 (11), 1813–1824.
Price, J.L., Drevets, W.C., 2010. Neurocircuitry of mood disorders. Neuropsychopharmacology 35 (1), 192–216.
Riva-Posse, P., Choi, K.S., Holtzheimer, P.E., McIntyre, C.C., Gross, R.E., Chaturvedi, A., Crowell, A.L., Garlow, S.J., Rajendra, J.K., Mayberg, H.S., 2014. Defining critical white matter pathways mediating successful subcallosal cingulate deep brain stimulation for treatment-resistant depression. Biol. Psychiatry 76 (12), 963–969.
Riva-Posse, P., Choi, K.S., Holtzheimer, P.E., Crowell, A.L., Garlow, S.J., Rajendra, J.K., McIntyre, C.C., Gross, R.E., Mayberg, H.S., 2018. A connectomic approach for subcallosal cingulate deep brain stimulation surgery: prospective targeting in treatment-resistant depression. Mol. Psychiatry 23 (4), 843–849.
Rosellini, A.J., Bourgeois, M.L., Correa, J., Tung, E.S., Goncharenko, S., Brown, T.A., 2018. Anxious distress in depressed outpatients: prevalence, comorbidity, and incremental validity. J. Psychiatr. Res. 103, 54–60.
Roy, A.K., Fudge, J.L., Kelly, C., Perry, J.S., Daniele, T., Carlisi, C., Benson, B., Castellanos, F.X., Milham, M.P., Pine, D.S., Ernst, M., 2013. Intrinsic functional connectivity of amygdala-based networks in adolescent generalized anxiety disorder. J. Am. Acad. Child Adolesc. Psychiatry 52 (3), 290–299 (e292).
Rush, A.J., Gullion, C.M., Basco, M.R., Jarrett, R.B., Trivedi, M.H., 1996. The inventory of depressive symptomatology (IDS): psychometric properties. Psychol. Med. 26 (3), 477–486.
Salimi-Khorshidi, G., Smith, S.M., Nichols, T.E., 2011. Adjusting the effect of non-stationarity in cluster-based and TFCE inference. Neuroimage 54 (3), 2006–2019.
Sexton, C.E., Mackay, C.E., Ebmeier, K.P., 2009. A systematic review of diffusion tensor imaging studies in affective disorders. Biol. Psychiatry 66 (9), 814–823.
Shen, X., Reus, L.M., Cox, S.R., Adams, M.J., Liewald, D.C., Bastin, M.E., Smith, D.J., Deary, I.J., Whalley, H.C., McIntosh, A.M., 2017. Subcortical volume and white matter integrity abnormalities in major depressive disorder: findings from UK biobank imaging data. Sci. Rep. 7 (1), 5547.
Smith, S.M., Nichols, T.E., 2009. Threshold-free cluster enhancement: addressing problems of smoothing, threshold dependence and localisation in cluster inference.

Neuroimage 44 (1), 83–98.
Smith, S.M., Jenkinson, M., Woolrich, M.W., Beckmann, C.F., Behrens, T.E., Johansen-Berg, H., Bannister, P.R., De Luca, M., Drobnjak, I., Flitney, D.E., Niazy, R.K., Saunders, J., Vickers, J., Zhang, Y., De Stefano, N., Brady, J.M., Matthews, P.M., 2004. Advances in functional and structural MR image analysis and implementation as FSL. Neuroimage 23, S208–S219 Suppl 1.
Smith, S.M., Jenkinson, M., Johansen-Berg, H., Rueckert, D., Nichols, T.E., Mackay, C.E., Watkins, K.E., Ciccarelli, O., Cader, M.Z., Matthews, P.M., Behrens, T.E.J., 2006. Tract-based spatial statistics: Voxelwise analysis of multi-subject diffusion data. Neuroimage 31 (4), 1487–1505.
Soares, J.M., Marques, P., Alves, V., Sousa, N., 2013. A Hitchhiker's guide to diffusion tensor imaging. Front. Neurosci. 7, 31.
Song, S.K., Sun, S.W., Ramsbottom, M.J., Chang, C., Russell, J., Cross, A.H., 2002. Dysmyelination revealed through MRI as increased radial (but unchanged axial) diffusion of water. Neuroimage 17 (3), 1429–1436.
Spalletta, G., Fagioli, S., Caltagirone, C., Piras, F., 2013. Brain microstructure of sub-clinical apathy phenomenology in healthy individuals. Hum. Brain Mapp. 34 (12), 3193–3203.
Stein, J.L., Wiedholz, L.M., Bassett, D.S., Weinberger, D.R., Zink, C.F., Mattay, V.S., Meyer-Lindenberg, A., 2007. A validated network of effective amygdala connectivity. Neuroimage 36 (3), 736–745.
Swartz, J.R., Monk, C.S., 2014. The role of corticolimbic circuitry in the development of anxiety disorders in children and adolescents. Curr. Top. Behav. Neurosci. 16, 133–148.
Van Essen, D.C., Ugurbil, K., Auerbach, E., Barch, D., Behrens, T.E., Bucholz, R., Chang, A., Chen, L., Corbetta, M., Curtiss, S.W., Della Penna, S., Feinberg, D., Glasser, M.F., Harel, N., Heath, A.C., Larson-Prior, L., Marcus, D., Michalareas, G., Moeller, S., Oostenveld, R., Petersen, S.E., Prior, F., Schlaggar, B.L., Smith, S.M., Snyder, A.Z., Xu, J., Yacoub, E., Consortium, W.U.-M.H., 2012. The human connectome project: a data acquisition perspective. Neuroimage 62 (4), 2222–2231.
van Tol, M.J., van der Wee, N.J.A., van den Heuvel, O.A., Nielen, M.M.A., Demenescu, L.R., Aleman, A., Renken, R., van Buchem, M.A., Zitman, F.G., Veltman, D.J., 2010. Regional brain volume in depression and anxiety disorders. Arch. Gen. Psychiatry 67 (10), 1002–1011.
Von Der Heide, R.J., Skipper, L.M., Klobusicky, E., Olson, I.R., 2013. Dissecting the uncinate fasciculus: disorders, controversies and a hypothesis. Brain 136, 1692–1707 Pt 6.
Wang, W., Qian, S., Liu, K., Li, B., Li, M., Xin, K., Sun, G., 2016. Reduced white matter integrity and its correlation with clinical symptom in first-episode, treatment-naive generalized anxiety disorder. Behav. Brain Res. 314, 159–164.
Wen, M.C., Steffens, D.C., Chen, M.K., Zainal, N.H., 2014. Diffusion tensor imaging studies in late-life depression: systematic review and meta-analysis. Int. J. Geriatr. Psychiatr. 29 (12), 1173–1184.
Westlye, L.T., Walhovd, K.B., Bjornerud, A., Due-Tonnessen, P., Fjell, A.M., 2009. Error-related negativity is mediated by fractional anisotropy in the posterior cingulate gyrus—a study combining diffusion tensor imaging and electrophysiology in healthy adults. Cereb. Cortex 19 (2), 293–304.
Westlye, L.T., Bjornebekk, A., Grydeland, H., Fjell, A.M., Walhovd, K.B., 2011. Linking an anxiety-related personality trait to brain white matter microstructure: diffusion tensor imaging and harm avoidance. Arch. Gen. Psychiatry 68 (4), 369–377.
WHO, 2017. Depression and Other Common Mental Disorders: Global Health Estimates. Geneva, Switzerland.
Wu, Y., Sun, D., Wang, Y., Wang, Y., Ou, S., 2016. Segmentation of the cingulum bundle in the human Brain: a new perspective based on DSI tractography and fiber dissection study. Front. Neuroanat. 10, 84.
Xia, W.P., Zhou, R.B., Zhao, G.Q., Wang, F., Mao, R.Z., Peng, D.H., Yang, T., Wang, Z.W., Chen, J., Fang, Y.R., 2018. Abnormal white matter integrity in Chinese young adults with first-episode medication-free anxious depression: a possible neurological biomarker of subtype major depressive disorder. Neuropsychiatr. Dis. Treat. 14, 2017–2026.
Zhao, K., Liu, H.Y., Yan, R., Hua, L.L., Chen, Y., Shi, J.B., Lu, Q., Yao, Z.J., 2017. Cortical thickness and subcortical structure volume abnormalities in patients with major depression with and without anxious symptoms. Brain Behav. 7 (8).
Zhu, X., Wang, X., Xiao, J., Zhong, M., Liao, J., Yao, S., 2011. Altered white matter integrity in first-episode, treatment-naive young adults with major depressive disorder: a tract-based spatial statistics study. Brain Res. 1369, 223–229.